

# Prediction of *in Vivo* Synergistic Activity of Antiangiogenic Compounds by Gene Expression Profiling<sup>1</sup>

Edith I. Cline, Silvio Biccato, Carlo DiBello, and Mark W. Lingen<sup>2</sup>

The Cardinal Bernardin Cancer Center, Loyola University Medical Center, Maywood, Illinois 60153 [E. I. C.]; Department of Chemical Process Engineering, University of Padova, Italy 35131 [S. B., C. D.]; and Department of Pathology, Division of Biological Sciences, Department of Pathology, The University of Chicago, Chicago, Illinois 60637 [M. W. L.]

## Abstract

Angiogenesis, an essential phenotype for tumor formation, requires the interaction of many cells within the tumor microenvironment. Therefore, successful antiangiogenic therapies must be able to block all of the different mechanisms tumors use to induce neovascularization. A major challenge for developing such protocols is determining which agents are likely to have the highest degree of synergistic activity *in vivo*. We treated human microvascular endothelial cells with six inhibitors of angiogenesis and used microarrays to seek divergent patterns of gene expression suggestive of potential synergies. The expression profiles of a thrombospondin-mimetic peptide (DI-TSPa) and TNP-470 (TNP) were very similar, whereas endostatin had a dramatically different profile. *In vitro*, endostatin was synergistically antiangiogenic with either TNP-470 or DI-TSPa. *In vivo*, mice bearing Lewis lung carcinoma cells treated with a combination of endostatin and either DI-TSPa or TNP-470, at doses that were ineffective when used alone, resulted in a marked inhibition of tumor growth and decreased tumor angiogenesis. Conversely, animals treated with both DI-TSPa and TNP-470 demonstrated a modest effect on both tumor growth and angiogenesis. These results suggest that even in the absence of a complete mechanistic understanding of how these inhibitors work, gene expression profiling may be used to predict synergistic antiangiogenic activity and thus maximize their antitumor efficacy.

## Introduction

Angiogenesis, the growth of new blood vessels from preexisting ones, is one of the essential phenotypes of physiological and pathologic conditions, including growth and development, wound healing, reproduction, arthritis, psoriasis, and neoplasia. In a series of now classical experiments, Folkman (1) demonstrated that solid tumors cannot grow >2–3 mm in diameter without being able to induce their own blood supply. Tumor growth can be stunted by a variety of single agents that have the common ability to inhibit angiogenesis (2), and recent reports suggested that combinational antiangiogenesis protocols can be more effective than single agent therapies (3–7). However, it is unclear which combinations of agents would be most efficacious. This is critically important for two reasons. Like other therapies, tumors may become resistant to individual antiangiogenic therapies, even those that target multiple angiogenic factors (8–10). In addition, antiangiogenic therapies must be designed to overcome the multitude of direct and indirect mechanisms by which tumors can induce new blood vessel growth, including eliciting the help of various stromal cells (11, 12). This study looks toward the long-term goal of identifying possible combinatorial antiangiogenic therapies that address

each of the possible mechanisms of tumor-induced angiogenesis, as well as reduce the likelihood of resistance.

## Materials and Methods

**Cell Culture and RNA Preparation.** HMVEC<sup>3</sup> (Cell Systems, Kirkland, WA) were cultured with endothelial growth media-microvascular media (Clonetics/BioWhittaker, Walkersville, MD). The cells were treated with one of each of the following agents: (a) all *trans*-RA (1  $\mu$ M; Sigma, St. Louis, MO); (b) recombinant IFN- $\alpha$  (50 IU/ml; Biosource International, Camarillo, CA); (c) PEDF (0.4 nM; a kind gift from Noel Bouck); (d) DI-TSPa (0.5 nM; Abbott Laboratories); (e) TNP-470 (1.5 nM; National Cancer Institute); and (f) ENDO (3 nM; National Cancer Institute) for 4 h. Total RNA was isolated from the cells using TRIzol reagent (Invitrogen, Carlsbad, CA). Lewis lung carcinoma cells were maintained in culture in DMEM supplemented with 10% heat-inactivated fetal bovine serum.

**Microarrays.** Human cDNA microarrays (Research Genetics/Invitrogen) consisted of nylon membranes containing 5295 named genes and 3889 ESTs (GF211 and GF205). The array also contained 576 spots of total genomic DNA that served as reference points for the image analysis software Pathways 2.0 (Research Genetics/Invitrogen) for normalization purposes to verify the homogeneity of the hybridization.

**Labeling, Hybridization, and Scanning of Microarray.** cDNA probes were made from 5  $\mu$ g of total RNA with  $\alpha$ [<sup>33</sup>P]-dATP (Amersham Biosciences, Piscataway, NJ) by oligo dT-primed polymerization using Super-Script II reverse transcriptase (Invitrogen). Probes were purified by gel chromatography (BioSpin 6; Bio-Rad Laboratories, Hercules, CA), boiled for ~3 min, and allowed to cool to room temperature. The microarrays were prehybridized for no <2 h and then hybridized overnight at 42°C. Filters were washed with 2  $\times$  SSC and 1% SDS for 15 min at 50°C and then with 0.5  $\times$  SSC and 1% SDS twice for a total of 30 min at room temperature. Washed filters were then exposed to phosphorimager screens, which were scanned by a Molecular Dynamics Storm Imager (Packard Instruments, Meriden, CT) at 600 dpi resolution. Scanned files containing the microarray were analyzed with Pathways software (Research Genetics/Invitrogen).

**Data Analysis.** To capture and characterize the genomic profiles of treated endothelial cells, the expression profile database was organized into a matrix in which the 9154 rows represented the genes and the ESTs (data observations) and six columns represented the different antiangiogenic agents (independent variables). The  $a_{ij}$ th element of the matrix accounts for the logarithm of the ratio between the expression levels of gene  $i$  in cells treated with agent  $j$  in normal conditions.

**Data Preprocessing.** Before inspecting the matrix to identify associations of some subset of the  $M$  genes (and their levels of expression) and the antiangiogenic agents, the database was preprocessed and standardized. Pathways 2.0 (Research Genetics/Invitrogen) and MathLab functions implemented according to Beissbarth procedure (13) and were used to quantify the background intensity and determine which genes are actually expressed. To compare the different experiments, the raw expression data were rescaled to

Received 8/28/02; accepted 10/29/02.

The costs of publication of this article were defrayed in part by the payment of page charges. This article must therefore be hereby marked *advertisement* in accordance with 18 U.S.C. Section 1734 solely to indicate this fact.

<sup>1</sup> Supported in part by NIH Grants DE12322 and DE00470 (M. W. L.).

<sup>2</sup> To whom requests for reprints should be addressed, at Division of Biological Sciences, Department of Pathology, The University of Chicago, 5841 South Maryland Avenue, MC 6101, Chicago, IL 60637. Phone: (773) 702-5548; Fax: (773) 702-9903; E-mail: mlingen@uchospitals.edu.

<sup>3</sup> The abbreviations used are: HMVEC, human microvascular endothelial cell; PC, principal component; PCA, principal component analysis; TNP, TNP-470; DEDD, death effector domain containing DNA binding protein; DI-TSPa, thrombospondin-mimetic peptide; MVD, microvessel density; RA, retinoic acid; EST, expressed sequence tag; ENDO, endostatin; PEDF, pigment epithelium-derived factor; VEGF, vascular endothelial growth factor; TRADD, tumor necrosis factor receptor-1 associated death domain.

account for different array intensities. Each column of the matrix has been multiplied by a factor of change, which was calculated such that the median of the ratios of intensities on a set of genes, that should have an equal or similar expression level in all of the experiments, becoming 1. This standardization is based on the expression levels of the 576 spots of total genomic DNA. After this preprocessing, gene expression values were subjected to a variation filter, which excluded genes showing minimal variation across the samples being analyzed. The variation filter tests for a fold change over samples, thus eliminating genes that did not show a relative change of  $\geq 3$ -fold for at least one of the six agents. The final database resulted in a 326 by six reduced matrix.

**Clustering.** We first created an empirical model that relates the correlational structure of the data to the various physiological states induced by the agent. Thus, to globally describe relationships among the different agents through the corresponding transcriptomes without losing the experimental information contained in the high-dimensional database, we first applied PCA on the reduced data set of 326 highly responsive genes. PCA reduces the dimensionality of complex data through a unitary transformation explained by an eigenvector and eigenvalue matrix. The columns of the eigenvector matrix are the PCs of the dataset, and the rows are the agents. The eigenvalues account for the overall variance that each component describes. Before developing the PCA, the data were normalized by standardizing each column (sample) to mean 0 and variance 1. PCA was implemented in MathLab using the singular value decomposition algorithm. To project, group, and visually inspect the six samples in a space describing the overall gene expression profiles, the coordinates of the first three PCs were analyzed. The use of PC1, PC2, and PC3 explains a reasonable amount of the total variance data ( $\sim 70\%$ ) and, at the same time, allows visual assessment of the clustering structure. To group transcripts sharing similar expression patterns, genes were clustered using hierarchical agglomerative clustering. Hierarchical clustering was performed using Cluster software on standardized data, and expression maps of clustered genes were created using TreeView.<sup>4</sup> Clusters were established using the clustering algorithm of Eisen *et al.* (14). This algorithm sorts through all of the data to find the pairs of genes that behave most similarly in each experiment and then progressively adds other genes to the initial pairs to form clusters of genes with potentially similar behavior. In the expression maps, each cell represents the expression ratio of a single transcript in a single sample; red and green represent ratios above and below, respectively, the median of the ratios for that gene across all of the samples. Color saturation is proportional to the magnitude of the difference from the average ratio.

**Endothelial Cell Migration Assay.** The endothelial cell migration assay was performed as described previously (15). Each substance was tested in quadruplicate in each experiment, and all experiments were repeated at least twice. VEGF (R&D Systems, Minneapolis, MN) was used as a positive control at a concentration of 100 pg/ml. The inhibitors of angiogenesis were used at the following concentrations in the migration assays: (a) all *trans*-RA (1  $\mu\text{M}$ ); (b) recombinant IFN- $\alpha$  (50 IU/ml); (c) PEDF (0.4 nM); (d) DI-TSPa (0.5 nM); (e) TNP-470 (1.5 nM); and (f) ENDO (3 nM). Optimal concentrations for VEGF and the six inhibitors were determined previously by dose-response experiments (data not shown).

**In Vivo Tumor Studies.** Lewis lung carcinoma cells were injected into the s.c. tissue of female 3–4-week-old *nu/nu* mice (Charles River Laboratories) at a final concentration of  $10^7$  cells in 0.1 ml. One group of mice was given s.c. injections of ENDO (2.5 or 20 mg/kg/day), DI-TSPa (20 or 30 mg/kg/day), and TNP-470 (10 or 30 mg/kg/day), respectively. *In vivo* maximal and  $\text{IC}_{50}$ s of each drug were determined in previous dose-response curve experiments (data not shown). A second group of mice was treated with a combination of ENDO and DI-TSPa, ENDO and TNP, and TNP-470 and DI-TSPa. A control group of mice was treated with PBS under the same conditions. Tumor growth was monitored over a period of 15 days by measurement with a caliper, and tumor volumes were calculated.

**Determination of *In Vivo* Microvessel Densities.** Formalin-fixed, paraffin-embedded tissue from each tumor was generated to quantify differences in vessel densities. MVD was assessed with the technique described previously (16) using biotin-conjugated rat antimouse CD-31 antibody (PharMingen, Los

Angeles, CA). Results were expressed as the highest number of microvessels observed at  $200\times$  in the “hot spot” region of each individual tumor.

## Results

**Global Expression Profiling of Antiangiogenic Agents.** To begin to define the global gene expression profiles of various inhibitors of angiogenesis, HMVECs were treated with either ENDO, a synthetic analogue of fungal protein (TNP-470), DI-TSPa, PEDF, RA, or IFN- $\alpha$ . RNA was isolated, labeled with  $^{33}\text{P}$ , and used to probe nylon filters containing a total of 9184 genes (5295 named and 3889 ESTs). Of these, 326 genes were significantly modulated with a  $\geq 3$ -fold induction or repression.

To test the hypothesis that it is possible to predict synergistic antiangiogenic activity based on gene expression profiling, we first created an empirical model that related the modulation of gene expression to the various physiological states induced by the agent. To globally describe relationships among the different agents through the corresponding transcriptomes without losing the experimental information contained in the high-dimensional database, we first performed a PCA. PCA reduces the dimensionality of complex data and displays the structure of sample interactions on a reduced space. The dimensional reduction is obtained through a linear transformation explained by a matrix, whose columns are the PCs (or the coordinates in the reduced space) of the data set and whose rows are the agents. We used the first three PCs, globally explaining  $\sim 70\%$  of the total variance, to project and group the six samples in a three-dimensional space. The PCA clustering of samples demonstrates that the six agents have a substantial separation, and four major groups can be identified (Fig. 1). In particular, ENDO and PEDF are largely separated from each other and from the remaining agents, whereas the couples TNP-DI-TSPa and IFN-RA tend to form two closely related clusters. These clustering results demonstrate four distinct expression patterns among the six inhibitors of angiogenesis and suggests that some of the inhibitors may act in a similar fashion. In addition, one might predict that inhibitors with different expression patterns would act by biologically divergent mechanisms.

**Prediction of Synergistic Antiangiogenesis Using Genomic Profiling.** From the results of the PCA, we hypothesized that inhibitors that modulated gene expression profiles in a similar fashion, such as TNP and DI-TSPa, would not be preferred candidates for synergistic antiangiogenic activity. Conversely, ENDO, because of its distinctly different profile, would be highly synergistic if combined with either

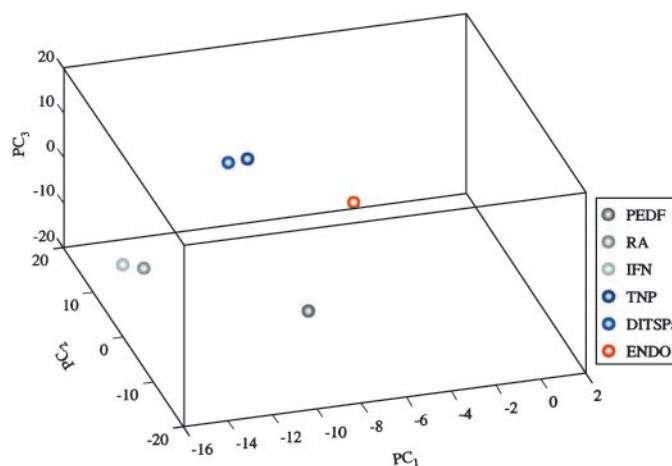


Fig. 1. PCA showing clustering of global expression profiles of endothelial cells treated with inhibitors of angiogenesis. This three-dimensional projection of the expression profiles reveals similarity of expression patterns by TNP and DI-TSPa, with a markedly different expression pattern for ENDO.

<sup>4</sup> Internet address: <http://rana.lbl.gov/EisenSoftware.htm>.

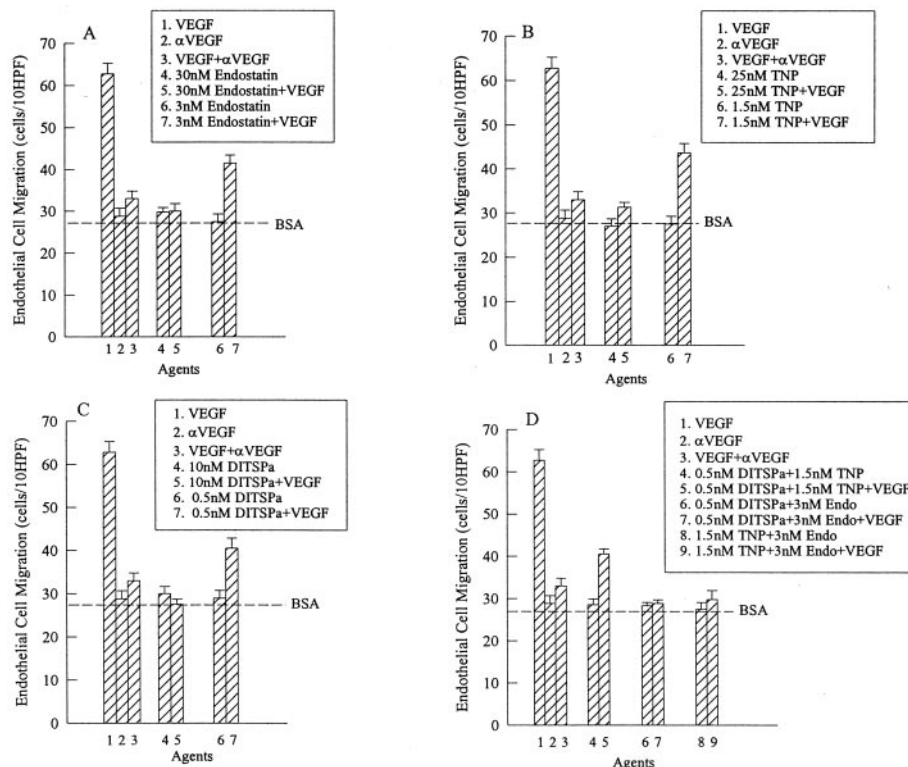


Fig. 2. Genomic profiling can be used to predict synergistic antiangiogenic activity in *in vitro* angiogenesis assays. HMVECs were assayed for the ability to migrate toward VEGF in the presence of different inhibitors of angiogenesis: (a) ENDO; (b) TNP-470; (c) DI-TSPa; and (d) various combinations of these agents. Compounds were tested at their maximal inhibitory and IC<sub>50</sub>s. Values are reported as the number of cells migrated per 10 high power fields.

TNP-470 or DI-TSPa. To test this hypothesis, we chose to focus on these three inhibitors (TNP, DI-TSPa, and ENDO). Using the endothelial cell migration assay, we tested the ability of ENDO, TNP-470, and DI-TSPa to inhibit the migration of HMVEC toward VEGF. We chose this assay as our screening method because we and others have found that this *in vitro* assay is a consistent predictor of *in vivo* angiogenesis. When used individually, the maximal *in vitro* inhibitory doses of ENDO, TNP, and DI-TSPa caused a marked inhibition of migration when compared with controls (Fig. 2). When the IC<sub>50</sub> of each inhibitor was tested in the migration assay, a lesser degree of inhibition was observed for the three agents (Fig. 2). However, the combination of the IC<sub>50</sub>s of ENDO with either TNP or DI-TSPa had a marked effect on cell migration (Fig. 2). Cells treated with as little as 3 nM of ENDO, combined with either 1.5 nM of TNP-470 or 0.5 nM of DI-TSPa, demonstrated the same level of inhibition of migration as cells treated with the maximum inhibitory doses of each of these individual agents (Fig. 2). The combined treatment of endothelial cells with the IC<sub>50</sub>s of TNP and DI-TSPa resulted in a modest effect.

To determine whether the observed *in vitro* synergies extended to the *in vivo* setting, we tested the ability of various combinations of ENDO, TNP-470, and DI-TSPa to slow the growth of Lewis lung carcinoma tumor cells in nude mice as well as decrease *in vivo* tumor angiogenesis. Tumor cells were injected into the flanks of nude mice, and tumors were allowed to grow to a size of 100 mm<sup>3</sup>. The mice were then treated with various doses of either ENDO, TNP-470, or DI-TSPa for 15 days. In addition, other groups of mice were treated with combinational therapy consisting of ENDO and TNP-470, ENDO and DI-TSPa, or TNP-470 and DI-TSPa for 15 days. The growth of Lewis lung primary tumors was suppressed by systemic doses of each of the individual agents. When used individually, the higher doses of ENDO, TNP, and DI-TSPa caused a marked reduction in tumor volume when compared with controls (Fig. 3). A lesser degree of inhibition of tumor growth was observed in the animals treated individually with the lower doses of ENDO, TNP, or DI-TSPa when compared with control animals. Importantly, the tumors from the animals treated con-

currently with ENDO and DI-TSPa or ENDO and TNP had markedly reduced mean tumor volumes, demonstrating a potent synergistic effect. In contrast, the combination of TNP and DI-TSPa resulted in a modest inhibition of tumor growth.

The observed inhibition of tumor growth in drug-treated animals was attributable at least in part to the antiangiogenic activity of these compounds. Animals treated individually with the full dosage of either TNP, DI-TSP, or ENDO had markedly decreased microvessel densities when compared with controls (Table 1). Animals treated individually with the IC<sub>50</sub>s of either TNP, DI-TSPa, or ENDO had modestly decreased vessel densities when compared with the controls (Table 1). Similarly, animals treated with the IC<sub>50</sub>s of the TNP/DI-TSPa combination therapy did not demonstrate a decrease in MVD over and above what was seen when using the IC<sub>50</sub> of either agent (TNP or DI-TSPa) alone. However, the mean MVD of the animals treated with the IC<sub>50</sub>s of TNP/ENDO and DI-TSPa/ENDO combinations was markedly reduced, with their vessels per hot spot being similar to areas seen in animals treated with the higher doses of each individual drug.

**Identification of Endothelial Cell Gene Expression Clusters.** To use expression patterns to identify potential mechanisms of action for these agents, we applied hierarchical agglomerative clustering, which groups genes according to the similarity of their expression profiles. Pearson correlation coefficient was used as a similarity measure. The agglomerative scheme revealed three major clusters of modulation: (a) ENDO up-regulation; (b) TNP and DI-TSPa up-regulation; and (c) ENDO down-regulation (Fig. 4A–C). These findings provide a potential road map for further investigation of genes that may contribute to the modulation of the angiogenic phenotype by these various agents.

**Discussion**

We have shown that genomic profiling can be used to identify antiangiogenic agents that have the greatest potential to work in a synergistic fashion based on their divergence in modulated endothelial



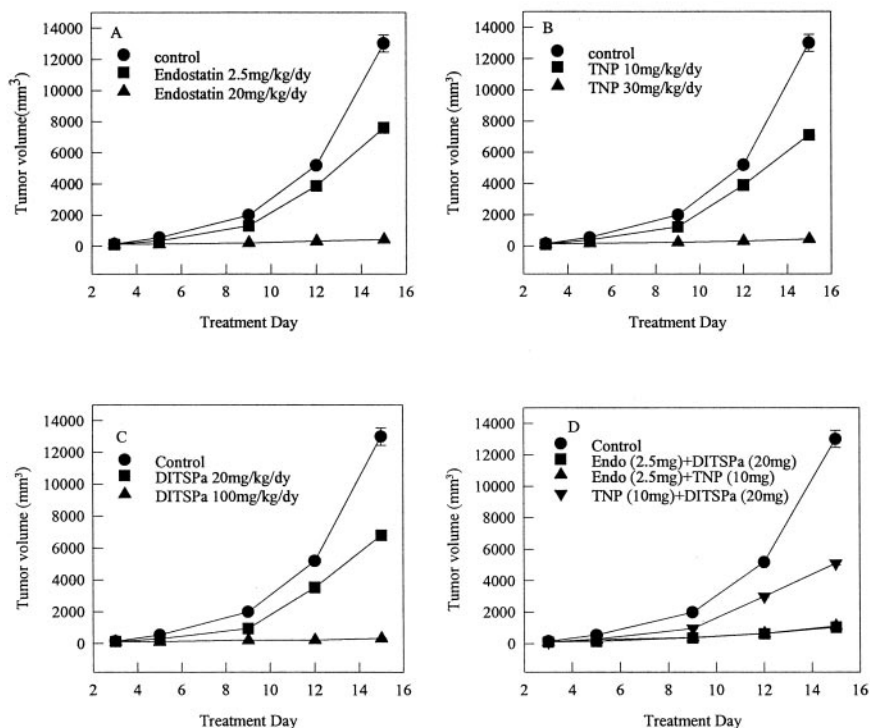


Fig. 3. ENDO acts synergistically *in vivo* to inhibit tumor growth when combined with either TNP-470 or DI-TSPa. Mice were implanted with Lewis lung carcinoma cells, and systemic therapy was begun when the tumors were ~100 mm<sup>3</sup>. Mice were treated with s.c. injections of ENDO (2.5 or 20 mg/kg/day), TNP-470 (10 or 30 mg/kg/day), or DI-TSPa (20 or 100 mg/kg/day) for 15 days. In addition, other groups of mice were treated with combinational therapy consisting of ENDO (2.5 mg/kg/day) and TNP-470 (10 mg/kg/day), ENDO (2.5 mg/kg/day) and DI-TSPa (20 mg/kg/day), or TNP-470 (10 mg/kg/day) and DI-TSPa (20 mg/kg/day) for 15 days. Control mice were treated with saline. Each data point represents the mean ± SE for five mice (n = 5).

cell gene expression. Specifically, we demonstrate that ENDO can act in a synergistic antiangiogenic fashion, both *in vitro* and *in vivo*, with either DI-TSPa or TNP-470, whereas the combination of DI-TSPa and TNP-470 did not. This observation comes at a critical juncture in the field of antiangiogenesis cancer therapy. There is a great deal of interest in developing chemotherapeutic clinical trials that are based on antiangiogenic therapies, with ~80 antiangiogenic agents being tested at this time. However, the results from a number of trials have been somewhat disappointing. Given the complexity of both the angiogenic phenotype and the challenges of treating patients with these agents, the initial findings of these trials should come as no surprise. Perhaps the greatest challenge for designing antiangiogenic therapies is that there are numerous direct and indirect mechanisms by which tumors can induce new blood vessel growth, including eliciting the help of various stromal cells. Therefore, it is reasonable to assume

that successful antiangiogenic protocols must address each of the possible mechanisms by which tumors can induce new blood vessel growth. We believe that the work presented here provides proof of principal and a working template that can be used to help prospectively design combinatorial antiangiogenic therapies that have a greater likelihood of eliciting a definable clinical response. The applicability of predictive genomic profiling for designing combinatorial antiangiogenic therapies against a number of different histological types of neoplasms is currently being evaluated.

In addition to identifying agents that may work in a synergistic antiangiogenic fashion, we have compiled a functional profile of genes whose expression was modulated and warrant further investigation to help elucidate the molecular mechanisms of these inhibitors. ENDO treatment of endothelial cells resulted in a 3–10-fold change in expression of 110 genes. Of these, a total of 38 were up-regulated, and 82 were down-regulated. There was some variability with regard to the class of genes whose expression was modulated. However, within this group, there was a number of genes that act as either transcription factors or inducers of apoptosis and cell cycle arrest. It has been proposed that ENDO inhibits angiogenesis by inducing apoptosis in activated endothelial cells (17) or by inhibiting endothelial cell migration in an apoptosis-independent fashion (18), and expression profiles provide support for each of these hypotheses.

Although ENDO modulated two unique clusters of genes (up- and down-regulated), a unique DI-TSPa/TNP cluster of up-regulated genes was also observed. A total of 35 genes was either induced or suppressed by both TNP-470 and DI-TSPa, some of which are reasonable candidates for participation in angiogenesis, *e.g.*, the Di-George syndrome (DGCR6L) gene, which is involved in abnormal embryonic blood vessel development (19), was up-regulated by both DI-TSPa and TNP-470.

Similar to ENDO, both TNP and DI-TSPa induced an up-regulation of death domain effectors. However, the specific genes that were modulated by each inhibitor were different. Although ENDO up-regulated TRADD and PML, DI-TSPa/TNP up-regulated the expression of a novel gene containing a death effector domain similar to that

Table 1 Synergistic inhibition of *in vivo* tumor angiogenesis by ENDO, TNP-470, and DI-TSPa

Treatment	MVD <sup>a</sup>
Control	110 ± 17
TNP	
(10 mg/kg/day)	45 ± 18
(30 mg/kg/day)	22 ± 9
DI-TSPa	
(20 mg/kg/day)	57 ± 17
(100 mg/kg/day)	16 ± 8
ENDO	
(2.5 mg/kg/day)	73 ± 7
(20 mg/kg/day)	27 ± 11
TNP/DI-TSPa	
(10 mg/kg/day TNP + 20 mg/kg/day DI-TSPa)	76 ± 9
TNP/ENDO	
(10 mg/kg/day TNP + 2.5 mg/kg/day ENDO)	28 ± 6
DI-TSPa/ENDO	
(20 mg/kg/day DI-TSPa + 2.5 mg/kg/day ENDO)	25 ± 9

<sup>a</sup> Mice bearing Lewis lung carcinoma cells were treated with s.c. injections of antiangiogenic agents as described above for 15 days. The tumors were then excised, fixed, and processed for determination of MVD. Data we reported as the mean MVD of individual 200× Fields counted from each tumor (n = 5 for each dosage tested), where the greatest amounts of neovascularization were observed.

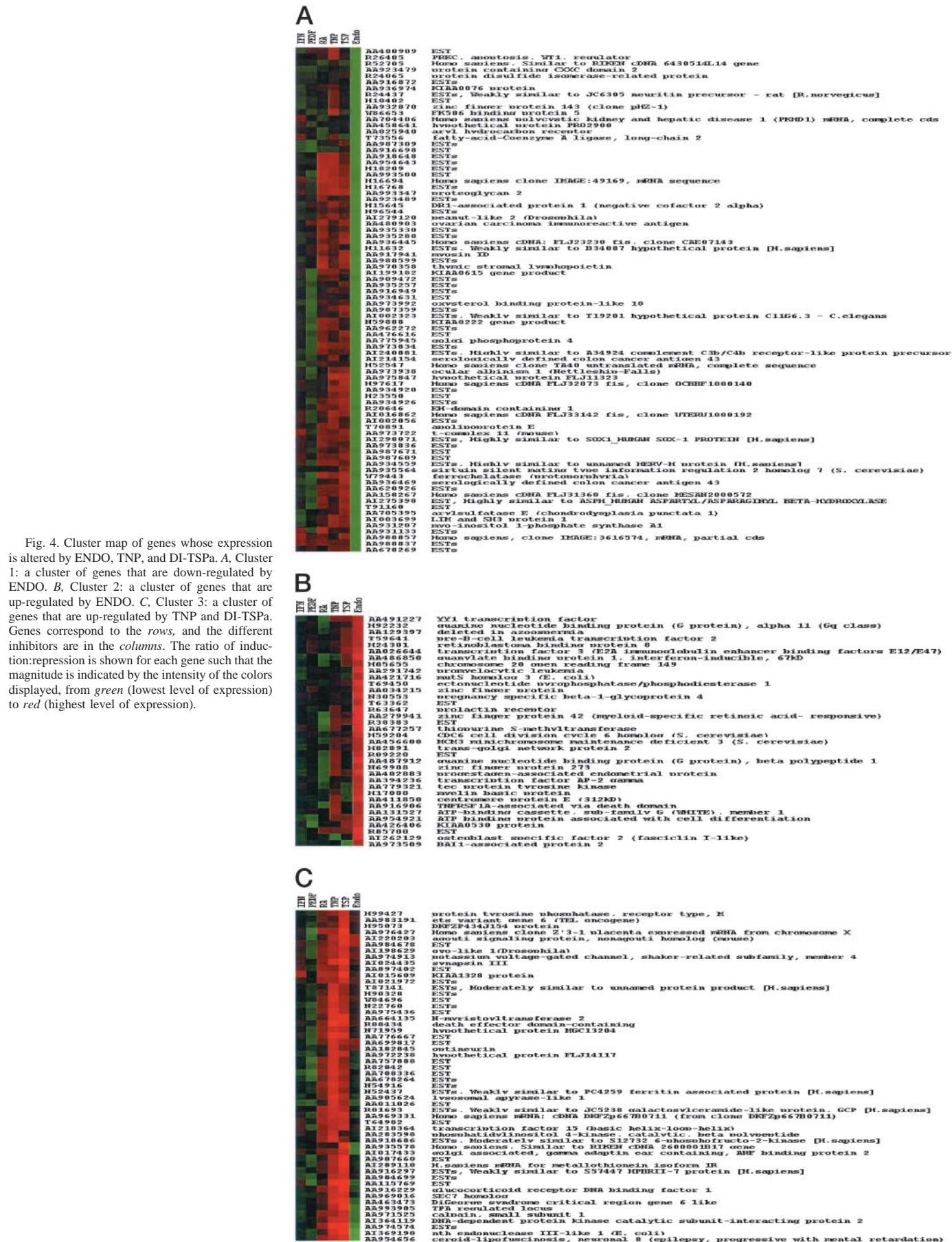


Fig. 4. Cluster map of genes whose expression is altered by ENDO, TNP, and DI-TSPA. A, Cluster 1: a cluster of genes that are down-regulated by ENDO. B, Cluster 2: a cluster of genes that are up-regulated by ENDO. C, Cluster 3: a cluster of genes that are up-regulated by TNP and DI-TSPA. Genes correspond to the rows, and the different inhibitors are in the columns. The ratio of induction:repression is shown for each gene such that the magnitude is indicated by the intensity of the colors displayed, from green (lowest level of expression) to red (highest level of expression).

found in DEDD. DEDD induces apoptosis by interacting with Fas-associated death domain and caspase 8, thereby shutting down transcription during Fas-mediated apoptosis (20). DEDD also colocalizes in the nucleus and causes the depression of RNA I polymerase transcription to induce apoptosis and shut off cellular biosynthetic activities (21). Therefore, although all three agents modulate genes related to apoptosis, the data suggest that the specific molecular mechanisms whereby each agent causes this phenomenon may be different.

The expression of the angiogenic phenotype in the tumor microenvironment is a DEDD complex process where the interplay between the tumor cells and various constituents of the surrounding normal stroma are thought to be critically important (11, 12). The work reported above suggests that genomic profiling can be used to identify which antiangiogenic agents are likely to work in a synergistic fashion in this complex and poorly understood environment and thereby guide clinical trials of these agents toward maximum efficacy. It also has the added benefit of identifying specific genes whose further study may be crucial to a detailed understanding of the molecular mechanisms that underlie the effectiveness of these promising therapeutic agents.

**References**

1. Folkman, J. Tumor angiogenesis. *In: J. Mendelsohn, P. M. Howley, M. A. Israel, and L. A. Liotta (eds.), The Molecular Basis of Cancer*, pp. 206–232. Philadelphia: W. B. Saunders, 1995.
2. Kerbel, R. S. Tumor angiogenesis: Past, present and the near future. *Carcinogenesis (Lond.)*, *21*: 505–515, 2000.
3. Brem, H., Gresser, I., Grosfeld, J., and Folkman, J. The combination of antiangiogenic agents to inhibit primary tumor growth and metastasis. *J. Ped. Surg.*, *28*: 1253–1257, 1993.
4. Lingen, M. W., Polverini, P. J., and Bouck, N. P. Retinoic acid and interferon alpha act synergistically as antiangiogenic and antitumor agents against head and neck squamous cell carcinoma. *Cancer Res.*, *58*: 5551–5558, 1998.
5. Mauceri, H. J., Hanna, N. N., Beckett, M. A., Gorski, D. H., Staba, M. J., Stellato, K., A. Bigelow, K., Heimann, R., Gately, S., Dhanabal, M., Soff, G. A., Sukhatme, V. P., Kufe, D. W., and Weichselbaum, R. R. Combined effects of angiostatin and ionizing radiation in antitumour therapy. *Nature*, *394*: 287–291, 1998.

6. Teicher, B. A. Potentiation of cytotoxic cancer therapies by anti-angiogenic agents. *In: B. A. Teicher (ed.), Anti-angiogenic Agents in Cancer Therapy*, pp. 277–316. Totowa, NJ: Human Press, Inc., 1999.
7. Minischetti, M., Vacca, A., Ribatti, D., Iurlaro, M., Ria, R., Pellegrino, A., Gasparini, G., and Dammacco, A. F. TNP-470 and recombinant human interferon-alpha2a inhibit angiogenesis synergistically. *Br. J. Hematol.*, *109*: 829–837, 2000.
8. Fidler, I. J. Angiogenic heterogeneity: regulation of neoplastic angiogenesis by the organ microenvironment. *J. Natl. Cancer Inst. (Bethesda)*, *93*: 1040–1041, 2001.
9. Filleur, S., Volpert, O. V., Degeorges, A., Volland, C., Reiher, F., Clezardin, P., Bouck, N., and Cabon, F. In vivo mechanisms by which tumors producing thrombospondin 1 bypass its inhibitory effects. *Genes Dev.*, *15*: 1373–1382, 2001.
10. Yu, J. L., Rak, J. W., Coomber, B. L., Hicklin, D. J., and Kerbel, R. S. Effect of p53 status on tumor response to antiangiogenic therapy. *Science (Wash. DC)*, *295*: 1526–1528, 2002.
11. Dvorak, H. F., Nagy, J. A., Dvorak, J. T., and Dvorak, A. M. Identification and characterization of the blood vessels of solid tumors that are leaky to circulating macromolecules. *Am. J. Pathol.*, *145*: 510–514, 1994.
12. Liss, C., Fekete, M. J., Hasina, R., Lam, C. K., and Lingen, M. W. Paracrine angiogenic loop between head and neck squamous cell carcinomas and macrophages. *Int. J. Cancer*, *93*: 781–785, 2001.
13. Beissbarth, T., Fellenberg, K., Brors, B., Arribas-Prat, R., Boer, J., Hauser, N. C., Scheideler, M., Hoheisel, J. D., Schutz, G., Poustka, A., and Vingron, M. Processing and quality control of DNA array hybridization data. *Bioinformatics*, *16*: 1014–1022, 2000.
14. Eisen, M. B., Spellman, P. T., Brown, P. O., and Botstein, D. Cluster analysis and display of genome-wide expression patterns. *Proc. Natl. Acad. Sci. USA*, *95*: 14863–14868, 1999.
15. Lingen, M. W., Polverini, P. J., and Bouck, N. P. Inhibition of squamous cell carcinoma angiogenesis by direct interaction of retinoic acid with endothelial cells. *Lab. Investig.*, *74*: 476–483, 1996.
16. Vermeulen, P. B., Gasparini, G., Fox, S. B., Toi, M., Martin, L., McCullouch, P., Pezzella, F., Viale, G., Weidner, N., Harris, A. L., and Dirix, L. Y. Quantification of angiogenesis in solid human tumors: an international consensus on the methodology and criteria of evaluation. *Eur. J. Cancer*, *32A*: 2474–2484, 1996.
17. Volpert, O. V., Zaichuk, T., Zhou, W., Reiher, F., Ferguson, T. A., Stuart, P. M., Amin, M., and Bouck, N. P. Inducer-stimulated Fas targets activated endothelium for destruction by anti-angiogenic thrombospondin-1 and pigment epithelium derived factor. *Nat. Med.*, *8*: 349–357, 2002.
18. Shichiri, M., and Hirata, Y. Antiangiogenesis signals by endostatin. *FASEB J.*, *15*: 1044–1053, 2001.
19. Towbin, J. A., Casey, B., and Belmont, J. The molecular basis of vascular disorders. *Am. J. Hum. Genet.*, *64*: 678–684, 1999.
20. Ashkenazi, A., and Dixit, V. M. Apoptosis control by death and decoy receptors. *Curr. Opin. Cell Biol.*, *11*: 255–260, 1999.
21. Stegh, A. H., Schickling, O., Ehret, A., Scaffidi, C., Peterhansel, C., Hofmann, T. G., Grummt, I., Krammer, P. H., and Peter, M. E. DEDD, a novel death effector domain-containing protein, targeted to the nucleolus. *EMBO J.*, *17*: 5974–5986, 1998.

# Cancer Research

The Journal of Cancer Research (1916–1930) | The American Journal of Cancer (1931–1940)

## Prediction of *in Vivo* Synergistic Activity of Antiangiogenic Compounds by Gene Expression Profiling

Edith I. Cline, Silvio Bicciato, Carlo DiBello, et al.

*Cancer Res* 2002;62:7143-7148.

**Updated version** Access the most recent version of this article at:  
<http://cancerres.aacrjournals.org/content/62/24/7143>

**Cited articles** This article cites 18 articles, 5 of which you can access for free at:  
<http://cancerres.aacrjournals.org/content/62/24/7143.full#ref-list-1>

**Citing articles** This article has been cited by 1 HighWire-hosted articles. Access the articles at:  
<http://cancerres.aacrjournals.org/content/62/24/7143.full#related-urls>

**E-mail alerts** [Sign up to receive free email-alerts](#) related to this article or journal.

**Reprints and Subscriptions** To order reprints of this article or to subscribe to the journal, contact the AACR Publications Department at [pubs@aacr.org](mailto:pubs@aacr.org).

**Permissions** To request permission to re-use all or part of this article, use this link  
<http://cancerres.aacrjournals.org/content/62/24/7143>.  
Click on "Request Permissions" which will take you to the Copyright Clearance Center's (CCC) Rightslink site.